

Improvement of direct determination of Cu and Mn in seawater by GFAAS and total elimination of the saline matrix with the use of hydrofluoric acid

J.Y. Cabon*

UMR CNRS 6521-UBO, 6 Avenue Le Gorgeu, BP 809, 29285 Brest-Cedex, France

Received 15 February 2004; received in revised form 4 June 2004; accepted 16 June 2004

Available online 28 August 2004

Abstract

Hydrofluoric acid, added to seawater, can assist in the removal of chloride in the drying step by precipitating fluoride salts, thus suppressing the chloride interference effects induced on the atomization signals of Cu and Mn. By adding HF to seawater before the analysis, MgF_2 and CaF_2 are precipitated at the bottom of the sampling flask, without precipitating Cu and Mn, and are consequently not introduced into the graphite furnace. Because sodium salts are eliminated at the pretreatment step, the whole seawater matrix is eliminated before the atomization of Cu or Mn. Therefore, the analyzed volume of seawater can be increased by using the multi-injection procedure without degradation of the limit of detection and risks of spectral interferences. The limit of detection obtained for Cu and Mn are 0.05 and $0.01 \mu\text{g L}^{-1}$, respectively, for a $50 \mu\text{L}$ analyzed seawater volume.

© 2004 Elsevier B.V. All rights reserved.

Keywords: Graphite furnace; Seawater; Cu, Mn, HF precipitation of Ca and Mg

1. Introduction

Due to the presence of a complex matrix, direct determination of elements in seawater is difficult. Indeed, the saline matrix induces spectral or non-spectral interferences that may lead to a severe degradation of the analytical signal. These problems have been partially solved with the use of different chemical modifiers, like NH_4NO_3 [1–7], HNO_3 [8–10], NaOH [11], organic acids [10,12,13] or various forms of palladium [14–16]. Most of these modifiers reduce interference effects and permit, in the case of Cu and Mn, to remove the major part of the seawater matrix (about 0.5 M Na species in seawater) before atomization. However, Mg and Ca species (0.06 M in seawater), still present at the atomization step, degrade the limit of detection. In previous papers, it has been shown that HF could be an interesting chemical modifier for

the determination of elements in sodium chloride medium [17] and in seawater [18,19]. Indeed, by precipitating insoluble Mg and Ca fluoride species at the drying step, it suppresses chloride interference effects and also permits to eliminate the major part of the saline matrix at the pretreatment step. However, when seawater and HF are added together into the furnace, refractory Mg and Ca species are still present at the atomization step and generate a background absorption signal limiting the volume that can be introduced into the furnace. Therefore, it appeared interesting to eliminate Mg and Ca species, through their precipitation as fluoride species in the sampling bottle, before GFAAS analysis.

2. Experimental

2.1. Instrument parameters and operation

A Perkin–Elmer 4100ZL was used for all atomic absorption measurements. End-capped pyrolytic-coated graphite

* Fax: +33 298017001.

E-mail address: Jean-Yves.Cabon@univ-brest.fr.

tubes equipped with integrated platforms were used. Samples were delivered to the furnace using a Perkin–Elmer AS-70 autosampler and stored in acid washed polypropylene cups prior to injection. The lamps used were Cr, Cu and Mn hollow cathode lamps (Perkin–Elmer); the respective analytical lines used were 357.9 nm, 324.8 nm and 279.5 nm. The inert gas was argon. Dilutions were carried out with calibrated Gilson Pipetman pneumatic syringes.

2.2. Ion chromatography

Sodium, magnesium and calcium were determined by ion chromatography after addition of hydrofluoric acid into seawater. The seawater solution was diluted a thousand times in water before analysis. The ion concentrations were measured with a Dionex DX-100 ion chromatograph. The ion chromatograph was equipped with a CS12 column and a cation self-generating suppressor CSRS-I; the eluent being 0.016 M methane sulfonic acid.

2.2.1. Reagents

Calibration solutions were prepared by dilution of 1 g L⁻¹ Cu or Mn in 0.5 M HNO₃ Merck standard. Hydrofluoric acid 40% (22.5 M) was suprapur grade (Merck). Ultrapure water from a Millipore mro-MQ system was used. The spiked seawater sample was a North Atlantic seawater sample, collected near Brest. Ten grams per liter Pd(NO₃)₂ in ~15% HNO₃ was a Merck product.

2.2.2. Seawater analysis

A National Research Council of Canada certified NASS-5 reference material (~0.5 M in chloride) was analyzed for validation of the analytical protocol. About 20 mL of NASS-5 seawater samples (weighed) were transferred to 30 mL clean polyethylene flasks. Two milliliters of 40% HF was then added into each flask. Samples were then stored for one night before analysis. Twenty microliters of 1 g L⁻¹ Pd(NO₃)₂ solution was pretreated at 1200 °C. Seawater sample was then directly pipetted from the top of the solution with the use of the autosampler. The electrothermal program used for the determination of Cu and Mn using 2 × 25 µL seawater sample is presented in Table 1. Blank values were 0.05 µg L⁻¹ for Cu and 0.06 µg L⁻¹ for Mn, respectively. A 5-s baseline offset compensation (BOC) time was used. The atomic signal was

recorded on a floppy disk. The data were then converted to ASCII format with the “peak data reformat” Perkin–Elmer software, and then transferred to Microsoft Excel 5 for mathematical post-treatments of the signal. A 2-s moving sum was used for peak area measurements.

3. Results and discussion

3.1. Precipitation study

When HF was added to seawater in the sampling flask, the precipitation of insoluble magnesium and calcium fluoride salts was observed. Their precipitation could be followed by GFAAS at the analytical line of Cr, i.e., 357.9 nm. Indeed, as previously observed by Katskov et al. [20], the vaporization of magnesium fluoride generates a strong MgF absorption band at 357.1 nm, close to the analytical line of chromium; consequently, we could use this analytical line to follow the precipitation of magnesium fluoride to the bottom of an autosampler cup, by pipetting with the autosampler from the upper part of the HF seawater solution. Indeed, at this analytical line, the background absorption signal generated by the vaporization of Na species (NaCl, NaF or Na oxides) is very low and the background absorption signal is mainly due to the presence of MgF. As shown in Fig. 1, the precipitation of MgF₂ is slow and highly dependent on HF concentration that is used. By adding an equal volume of 22.5 M HF to seawater, it can be noted that the background absorption signal is drastically reduced after about 2 h; ion chromatographic measurements confirmed that Mg and Ca were practically removed from the solution. By adding an equal volume of 2.5 M HF, the precipitation of magnesium fluoride is much slower; magnesium and calcium are removed from the solution after a much longer time. From these observations, it appears that Ca and Mg can be removed from seawater by precipitation of fluoride species leading to a less refractory matrix.

Because this solution, to simplify the seawater matrix for the determination of elements, can be used only if they are not co-precipitated with fluoride salts, we examined the behavior of Cu and Mn during the precipitation of magnesium and calcium fluoride salts for different [HF] to [Cl⁻] mole concentration ratios. To examine the influence of magnesium and calcium fluoride precipitation on the stability

Table 1
Graphite atomizer program for the analysis of certified reference seawater

	Step								
	1	2	3 ^a	4 ^a	5 ^a	6	7	8	9
Introduction	Pd(NO ₃) ₂	Sample							
Temperature (°C)	130	1200	130	160	1250	1350	20	2300	2500
Ramp time (s)	5	10	1	60	10	5	1	0	1
Hold time (s)	30	30	5	5	30	60	10	5	5
Read								On	
Ar flow rate (mL min ⁻¹)	250	250	250	250	250	250	250	0	250

^aRepeated steps.

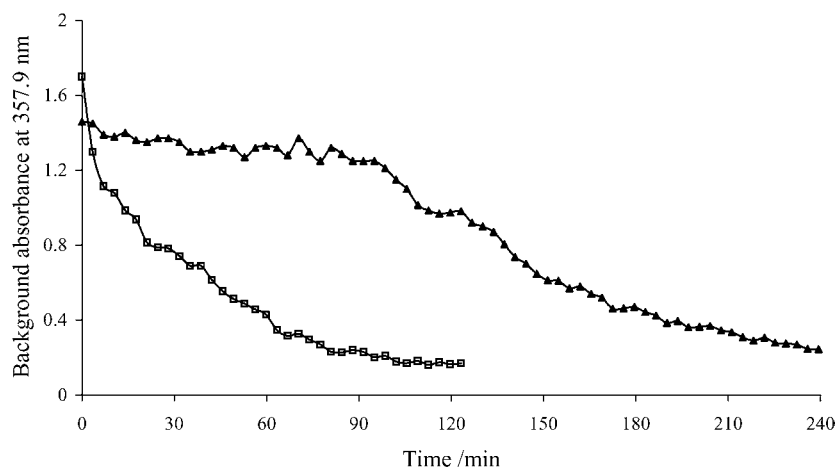


Fig. 1. Variation with time of MgF absorbance at 357.9 nm in seawater, mixed into an autosampler cup with an equal volume of 2.5 M HF (\blacktriangle) or 22.5 M HF (\square); 10 μ L; $T_{\text{atom}} = 2300^\circ\text{C}$.

of Cu and Mn in HF seawater solutions, we followed the variation of their relative integrated absorbance with time. The chloride interference effects observed for [HF] to $[\text{Cl}^-]$ mole concentration ratios below 10 decreases with time, particularly for Cu (Fig. 2, left). The chloride interference ($\sim 50\%$ for Cu and $\sim 15\%$ for Mn) is practically suppressed for a 10% HF seawater solution after 3 days mixing. The decrease of the integrated absorbance observed for Mn at high HF concentrations may be attributable to a slow partial precipitation or to an adsorption process of manganese species on the fluoride precipitate (Fig. 2, right). This phenomenon was not observed for Cu, even after 15 days. From this study, a [HF] to $[\text{Cl}^-]$ mole concentration ratio of about 10 appears adequate for the determination of Cu and Mn because it minimizes the interference effects and no removal of Cu or Mn from the solution is observed. Moreover, the relatively low volume of HF used permits to increase the seawater volume that can be introduced into the atom-

izer through a single injection and to minimize the blank value.

3.2. Optimization of experimental conditions

Due to the numerous parameters to be optimized in GFAAS, the a priori calculation of the limit of detection with the use of L'vov equation is an interesting tool to optimize spectroscopic and electrothermal parameters and data treatment [21]. The mass detection limit for our Perkin–Elmer apparatus is expressed by the following relation [18,19]:

$$m_L = 3 \times 0.046 \times 10^{(-E/36)} \frac{1}{\sqrt{54}} \frac{m}{Q_A} t_{\text{int}} \sqrt{\frac{10 \tilde{A}_{\text{BG}}}{t_{\text{int}}} + \frac{1}{t_{\text{boc}}}} \quad (1)$$

E is the parameter that is displayed on the Perkin–Elmer 4100ZL spectrometer; Q_A the integrated absorbance; m the

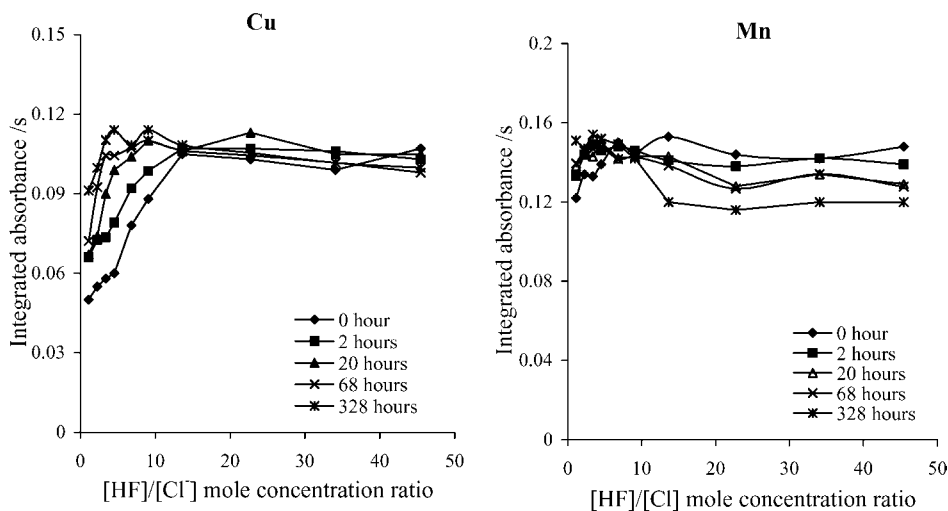


Fig. 2. Variation of the relative integrated absorbance of Cu (left) and Mn (right) with [HF] to $[\text{Cl}^-]$ mole concentration ratio for different reaction times. 5 μ L; $T_{\text{pret}} = 1250^\circ\text{C}$ (60 s); $T_{\text{atom}} = 2300^\circ\text{C}$.

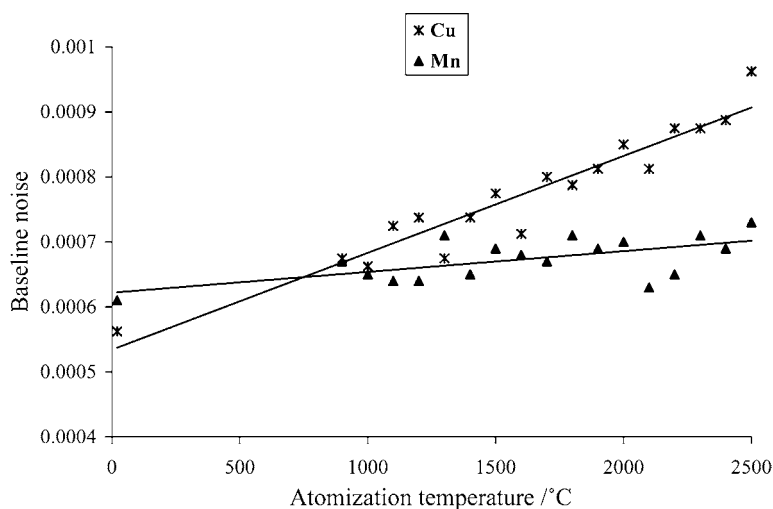


Fig. 3. Variation of the baseline noise with the atomization temperature for Cu and Mn.

mass of analyte; t_{int} the integration time; t_{boc} the baseline offset compensation time; \tilde{A}_{BG} the weighted mean background absorption signal.

3.2.1. Spectroscopic conditions

At the recommended lamp current, a two times lower limit of detection was obtained in the case of Cu with a 2 nm spectral bandwidth instead of the recommended 0.7 nm spectral bandwidth. In the case of Mn, the recommended 0.2 nm spectral bandwidth led to a much higher sensitivity but, on the other hand, to a three times poorer detection limit than the 2 nm spectral bandwidth.

3.2.2. Pretreatment temperature

In the 10% HF seawater medium, pretreatment curves of Cu are similar, with or without the use of palladium. For Mn, the remaining fluoride interference effect is suppressed

by using a pretreatment step at about 1300 °C. For Cu and Mn, a pretreatment step at about 1300 °C permits to eliminate sodium salts. In these conditions, due to the absence of Mg and Ca species, atomization of Cu and Mn can be performed in total absence of absorbing matrix (i.e., $\tilde{A}_{\text{BG}} = 0$) when Pd is not used.

3.2.3. Atomization temperature

The limit of detection is dependent on signal duration (t_{int}) and magnitude (Q_A) that varies with the atomization temperature. Moreover, the atomization temperature may have an influence on the baseline noise, and consequently on the limit of detection. As shown in Fig. 3, the increase of the baseline noise with the atomization temperature is relatively small in the case of Mn but, in the case of Cu, its increase with the atomization temperature is more important, i.e., about two times higher than the noise measured at 25 °C (in good

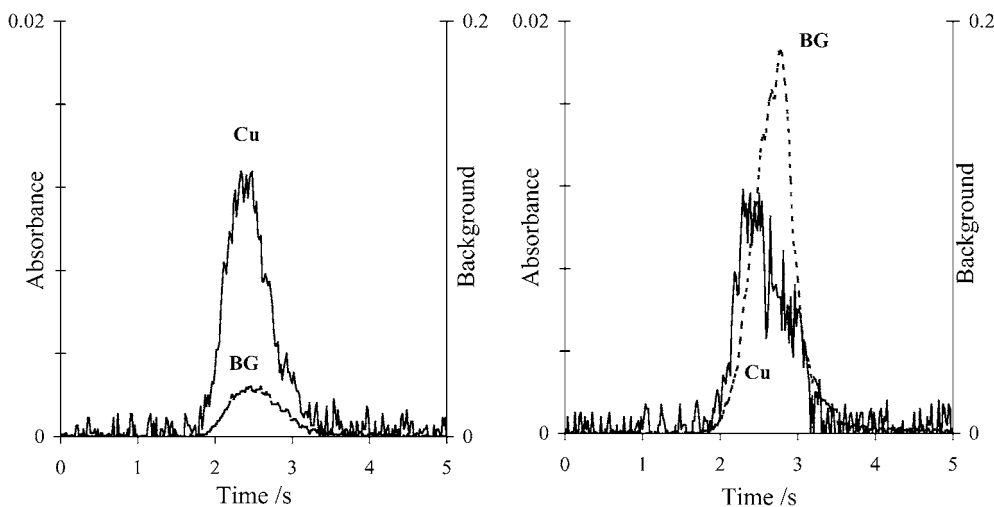


Fig. 4. Atomization signal of Cu in 50 μL ($2 \times 25 \mu\text{L}$) seawater supernatant 10 % in HF: after 3 days precipitation (left) or introduced as the mixture of the precipitate with seawater supernatant (right). Repeated steps (drying + pretreatment (1200 °C, 30 s)). $T_{\text{pret}} = 1350$ °C (60 s); $T_{\text{atom}} = 2400$ °C; 20 μg Pd introduced as $\text{Pd}(\text{NO}_3)_2$, pretreated at 1200 °C, 30 s.

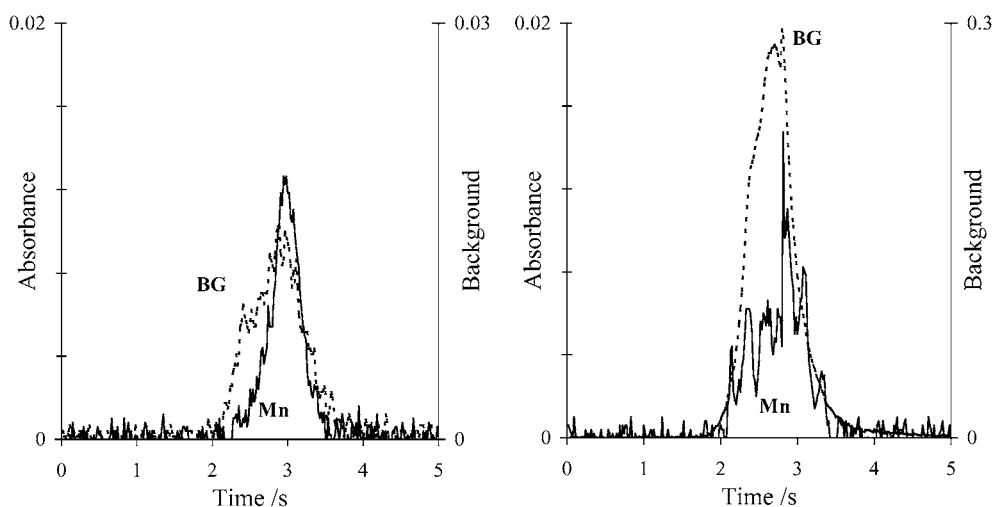


Fig. 5. Atomization signal of Mn in 50 μL ($2 \times 25 \mu\text{L}$) seawater supernatant 10% in HF: after 3 days precipitation (left) or introduced as the mixture of the precipitate with seawater supernatant (right). Repeated steps (drying + pretreatment (1250°C , 30 s)). $T_{\text{pret}} = 1350^\circ\text{C}$ (60 s); $T_{\text{atom}} = 2400^\circ\text{C}$; 20 μg Pd introduced as $\text{Pd}(\text{NO}_3)_2$, pretreated at 1200°C , 30 s.

agreement with the calculated noise value from L'vov equation). This increase is due to the contribution of the thermal emission of the tube walls, dependent on wavelength, temperature, optical path and furnace geometry. Consequently, to optimize the atomization temperature, it appears more recommendable to use the experimental baseline noise value $\sigma_{T_{\text{atom}}}$ determined at the atomization temperature (that includes the 4.2–4.3 Hz cyclic noise contribution observed for the 4100ZL spectrometer [22–24]) than the $0.046 \times 10^{(-E/36)}$ expression used in Eq. (1). Using this modified equation, the lower limits of detection for Cu and Mn are obtained for atomization temperatures higher than 2200°C ($\sim 30\%$ lower than with the use of the recommended atomization temperatures, i.e., 2000°C for Cu and 1900°C for Mn).

3.2.4. Sample volume

The variations of the integrated absorbance of Cu with the applied seawater volume (5 μL to $4 \times 25 \mu\text{L}$) were linear and similar to the analytical curves obtained in water. When Pd was not used, a curvature was observed for volumes higher than 25 μL . In the case of Mn, the variations of the integrated absorbance with the analyzed seawater volume were similar, with or without the use of Pd. However, a slight curvature as compared to water could be observed for volumes higher than $2 \times 25 \mu\text{L}$.

3.2.5. Application

The atomization signal of Cu obtained in optimized experimental conditions is presented in Fig. 4 (left). This figure shows clearly the improvement obtained by the complete removal of the background absorption signal generated by the vaporization of magnesium and calcium fluoride species (Fig. 4, right). Consequently, all the risks of spectral interferences are eliminated. A similar improvement is observed

in the case of Mn in the absence of Mg and Ca species (Fig. 5). The background absorption signal practically disappears when Pd is not added.

The experimental limits of detection (3σ , 20 measurements) obtained for Cu and Mn are $0.05 \mu\text{g L}^{-1}$ and $0.01 \mu\text{g L}^{-1}$, respectively, for a 50 μL analyzed seawater volume.

The respective concentrations of Cu and Mn determined in NASS-5 certified seawater were $0.275 \pm 0.007 \mu\text{g L}^{-1}$ and $0.91 \pm 0.01 \mu\text{g L}^{-1}$ for $0.297 \pm 0.046 \mu\text{g L}^{-1}$ and $0.919 \pm 0.057 \mu\text{g L}^{-1}$ certified values, respectively (at the 95% confident level, 5 measurements). No significant concentration variations were observed after a two-month storage in a 10% HF seawater solution.

References

- [1] R.E. Sturgeon, S.S. Berman, A. Desaulniers, D.S. Russell, *Talanta* 27 (1980) 85–94.
- [2] R.D. Ediger, G.E. Peterson, J.D. Kerber, *At. Absorpt. Newslett.* 13 (1974) 61–64.
- [3] J.M. Mac Arthur, *Anal. Chim. Acta* 93 (1977) 77–83.
- [4] R.E. Sturgeon, S.S. Berman, J.A.H. Desaulniers, D.S. Russell, *Anal. Chem.* 51 (1979) 2364–2369.
- [5] M. Hoenig, R. Wollast, *Spectrochim. Acta* 37B (1982) 399–415.
- [6] S.D. Huang, K.Y. Shih, *Spectrochim. Acta* 48B (1993) 1451–1460.
- [7] M.-S. Chan, S.-D. Huang, *Talanta* 51 (2000) 373–380.
- [8] G.R. Carrick, W. Slavin, D.C. Manning, *Anal. Chem.* 53 (1981) 1866–1872.
- [9] J.Y. Cabon, A. Le Bihan, *Anal. Chim. Acta* 198 (1987) 103–111.
- [10] J.Y. Cabon, A. Le Bihan, *Spectrochim. Acta* 50B (1995) 1703–1716.
- [11] C.-H. Lan, Z.B. Alfassi, *Analyst* (1994) 119.
- [12] S. Xiao-quan, B. Radziuk, B. Welz, O. Vyskocilova, *J. Anal. At. Spectrom.* 8 (1993) 409–413.
- [13] M. Tominaga, K. Bansho, Y. Umetsaki, *Anal. Chim. Acta* 169 (1985) 171–177.

- [14] G. Schlemmer, B. Welz, *Spectrochim. Acta* 41B (1986) 1157–1165.
- [15] S.-D. Huang, W.-R. Lai, K.-Y. Shih, *Spectrochim. Acta* 50B (1995) 1237–1246.
- [16] C.-L. Chen, S.-K. Danadurai, S.-D. Huang, *J. Anal. At. Spectrom.* 16 (2001) 404–408.
- [17] I. Lopez-Garcia, M. Sanchez-Medos, M. Hernandez-Cordoba, *Anal. Chim. Acta* 396 (1999) 279–284.
- [18] J.Y. Cabon, *Spectrochim. Acta* 57B (2002) 513–524.
- [19] J.Y. Cabon, *Spectrochim. Acta* 57B (2002) 939–950.
- [20] D.A. Katskov, R.M. Mofolo, P. Tittarelli, *Spectrochim. Acta* 55B (2000) 1577–1590.
- [21] B.V. L'vov, L.K. Polzik, A.V. Borodin, A.O. Dyakov, A.V. Novichikin, *J. Anal. At. Spectrom.* 10 (1995) 703–709.
- [22] J.Y. Cabon, A. Le Bihan, *Spectrochim. Acta* 50B (1995) 1703–1714.
- [23] M.T.C. de Loos-Vollebregt, E.X. Vrouwe, *Spectrochim. Acta* 52B (1997) 1341–1349.
- [24] S. Tang, P.J. Parsons, W. Slavin, *Spectrochim. Acta* 52B (1997) 1351–1365.